ELSEVIER

Journal of Molecular Structure 356 (1995) 169–182

Journal of
MOLECULAR
STRUCTURE

FT-IR, UV–visible and X-ray studies of complexes of pyridine *N*-oxides with pentachlorophenol

Zofia Dega-Szafran, Monika Grundwald-Wyspiańska, Anna Kania, Zofia Kosturkiewicz, Ewa Tykarska, Mirosław Szafran*

Faculty of Chemistry, A Mickiewicz University, 60780 Poznan, Poland

Received 5 September 1994; accepted in final form 23 May 1995

Abstract

The crystal structure of the 4-methoxy-2,6-dimethylpyridine *N*-oxide·pentachlorophenol complex has been determined by X-ray analysis. The O···O distance is 2.439(6) Å, the OHO angle is 152.3° and the hydrogen-bonded proton is close to the phenol molecule. The FT-IR spectra of pentachlorophenol complexes with some substituted pyridine *N*-oxides in the solid state and seven aprotic solvents of different polarity (ϵ from 2.27 to 37.5) show a broad absorption. The broad absorption shows weak dependence upon solvent polarity and is classified as type (ii). UV spectra show that in the investigated complexes protons are not transferred from the phenol to the *N*-oxides. Formamide ($\epsilon = 111$) is a much stronger proton acceptor than the pyridine *N*-oxides. Pentachlorophenol in formamide is converted to the phenolate ion.

1. Introduction

Pyridines with some carboxylic acids [1] and phenols [2] and pyridine *N*-oxides with some carboxylic acids [1] form AHB complexes containing strong hydrogen bonds, which are characterized by high enthalpies [3] ($\Delta H \approx 9$–22 kcal mol^{-1}), short A–B equilibrium distances [1,2(b)] ($R_{A-B} < 2.6$ Å), and a spectacular broad (continuous) absorption in the 3000–400 cm^{-1} region. The profile of the broad absorption exhibits a characteristic structure in some complexes; the subbands are generally denoted as A, B, C, D and E bands ($A > 2800$, B ≈ 2500, C ≈ 1900, D ≈ 1100 and E ≈ 850 cm^{-1}). Resonance of the hydrogen-bonded protons is strongly deshielded.

The profiles of the broad absorption in solution can be reproduced theoretically by assuming that there are complex relaxation processes in which several oscillators, coupled by anharmonic forces, are simultaneously relaxing [4–8].

Contrary to the widely investigated complexes of pyridines with phenols, complexes of pyridine *N*-oxides have not been studied systematically. To our knowledge only a few data are available [9]. Pyridine *N*-oxides with pentachlorophenol, HPCP, ($pK_a = 4.5$ [10(a)], 4.82 [10(b)] form two types of complexes with 1:1 and 2:1 acid/base ratios. In this paper we describe the 1:1 complexes and discuss the prototropic equilibrium (A–H···B $\rightleftarrows$ A$^-$···H–B$^+$), widely postulated in the literature for phenol complexes.

* Corresponding author.

SSDI 0022-2860(95)08954-3

Table 1
Melting points and elemental analyses of complexes of substituted pyridine *N*-oxides with pentachlorophenol and tetrabutylamino-pentachlorophenolates

No.	Substituent	pK_a	M.p. (°C)	Formula	Found (%)			Required (%)		
					C	H	N	C	H	N
1	4-Cl	0.36	147	$C_{11}H_5NO_2Cl_6$	33.35	1.44	3.69	33.37	1.27	3.54
2	H	0.79	125	$C_{11}H_6NO_2Cl_5$	36.47	1.55	3.90	36.55	1.67	3.88
3	3,5-Me_2	1.23	110–111	$C_{12}H_8NO_2Cl_5$	39.82	2.76	3.59	40.09	2.59	3.60
4	4-OMe-2,6-Me_2	3.45	115	$C_{14}H_{12}NO_3Cl_5$	40.11	3.19	3.44	40.08	2.88	3.34
5	4-NMe_2-2,6-Me_2	4.75	193–194	$C_{15}H_{15}N_2O_2Cl_5$	41.42	3.48	6.49	41.65	3.50	6.48
6	Bu_4N · PCP		105–106	$C_{22}H_{36}NOCl_5$	51.90	6.91	2.93	52.04	7.15	2.76
7	Bu_4N · (PCPHPCP)		92–93	$C_{28}H_{37}NO_2Cl_{10}$	43.49	4.91	1.99	43.44	4.82	1.91

2. Experimental

Complexes were prepared by adding stoichiometric amounts of HPCP to hot acetonitrile solutions of pyridine *N*-oxides. After cooling, the resulting precipitates were recrystallized from acetonitrile. Tetrabutylammonium pentachlorophenolate, salt **6**, was obtained by mixing equimolar amounts of n-Bu_4NOH (about 40% aq.) and HPCP; the product was extracted with chloroform, the organic layer was dried with Na_2SO_4, and the solvent removed by evaporation. The remaining solid was recrystallized from ethyl acetate. Tetrabutylammonium hydrogen dipentachlorophenolate, salt **7**, was prepared by dissolving the equivalent amount of salt **6** and HPCP in ethyl acetate. Melting points, elemental analyses and numbering of the investigated complexes are given in Table 1.

Solvents were purified by standard methods and stored over molecular sieves (4 or 3 Å).

The FT-IR spectra were measured at 2 cm^{-1} resolution using a Bruker IFS 113v instrument, which was evacuated to avoid water and CO_2 absorptions. Each spectrum consists of 250 scans at 31° in a cell with KBr windows, 0.1 and 0.25 mm thick. A standard solution of a crystalline complex was 0.1 mol dm^{-3}. The solid-state spectra were measured as suspensions in Nujol and poly(chlorotrifluoroethylene). Centre of gravities, $\nu' = \int \nu \log(I_0/I)\, d\nu / \int \log(I_0/I)\, d\nu$, were obtained by numerical integration with $d\nu = 0.964$ cm^{-1}.

UV-visible spectra were determined on a Specord M-40 Carl Zeiss Jena spectrometer in two different cells, $l = 0.1$ cm, $c \approx 5 \times 10^{-4}$ mol dm^{-3} and $l = 0.0029$ cm, $c = 0.05$ mol dm^{-3}. The high concentration was used to minimize the amount of "free" HPCP in solution. The solid-state spectra were measured in a KBr disc and in Nujol.

Crystal data, details concerning data collection and structure refinement are given in Table 2. Intensity data were collected on a KM-4 diffractometer using graphite-monochromated Cu $K\alpha$ radiation. Two check reflections (023, 032) recorded every 100 measurements showed maximum intensity variation of 3.5%. The intensities were corrected for Lorentz and polarization factors, and prepared for further calculations by DATARED [11] from the KM-4 package. The structure was solved by direct methods using the SHELXS-86 program [12]. All hydrogen atoms were located from the geometry, except for the hydrogen-bonded proton, which was located on the difference Fourier map. The parameters of non-hydrogen atoms were refined by a full-matrix least-squares procedure with anisotropic displacement factors and only B_{iso} was refined for hydrogen atoms using the program SHELX-76 [13]. The structure factors were corrected for extinction according to $F^* = F(1 - 0.0001\, xF^2/\sin\theta)$ where x refined to 0.065(4). Atomic scattering factors were taken from the International Tables for X-ray Crystallography [14].

Table 2
Crystallographic data and experimental details

Crystal data	
Molecular formula	$C_{14}H_{12}Cl_5NO_3$
Molecular weight	419.5
Crystal habit	Colourless prism
Crystal size (mm)	0.20 × 0.25 × 0.40
Crystal system	Triclinic
Space group	$P\bar{1}$
Unit cell parameters	
a (Å)	7.765(1)
b (Å)	9.377(1)
c (Å)	12.566(2)
α (deg)	91.13(1)
β (deg)	106.25(1)
γ (deg)	90.69(1)
V (Å^3)	878.1(4)
Z	2
D_x	1.587
Wavelength (Å)	1.54178
Absorption coefficient (mm^{-1})	7.642
Reflections for lattice parameters calculations	25
2θ range (deg)	24.9–62.2
Temperature (K)	292
Data collection	
Diffractometer type	KM-4
Collection method	ω–2θ
Number of reflection measured	3004
Number of independent reflections	2855
Number of observed reflections	2262
Criterion for observed	$F_0 \geqslant 4.0\sigma(F)$
$2\theta_{max}$ (deg)	1.0 to 130.0
R_{int}	0.0378
Index ranges	$-9 \leqslant h \leqslant 8$
	$-11 \leqslant k \leqslant 11$
	$0 \leqslant l \leqslant 14$
Refinement	
Number of parameters	221
Number of reflections used in refinement	2262
Function minimized	$\sum w(F_0 - F_c)^2$
Weighting scheme, g	0.00015
$w^{-1} = \sigma^2(F) + g(F)^2$	
R	0.0716
R_w	0.0829
S	2.72
$(\Delta/s)_{max}$	0.001
$(\Delta\rho)_{min}$(e Å^{-3})	−0.48
$(\Delta\rho)_{max}$(e Å^{-3})	0.58

3. Results and Discussion

3.1. IR spectra

In the solid-state IR spectra of the investigated complexes (Fig. 1) a broad absorption, as expected, strongly depends on the proton-acceptor properties of the *N*-oxides. In complex **1** (the weakest base) bands A and B are the most intense, whereas bands C and D are weak. On increasing the pK_a values of the *N*-oxides, the intensity of bands A and B decreases and simultaneously the intensity of bands D and E increases. In complex **4** bands B and C are very weak and bands D and E are very strong. Further increases of basicity caused the intensity of bands B–E changes to reverse, as in complex **5**. The observed changes of the broad absorption with the proton-acceptor properties of the pyridine *N*-oxides reflect variation of the O···O distance. These data suggest that the shortest bonds are in complexes **4** and **5** and X-ray results confirmed this conclusion (see below).

Calorimetric measurements demonstrate that in solution there are dipolar and specific interactions between the phenol–pyridine complex and solvents [3(c,d)]. In the investigated complexes the dipolar interaction can be estimated from the variation of the broad absorption, but the specific interaction can be determined from the intensity and frequency of absorption in the 3550–3250 cm^{-1} region due to the νOH···Solv. vibration (Fig. 1). The following values of the νOH···Solv. vibration were found: benzene, 3489 cm^{-1}; tetrachloroethylene, 3522 cm^{-1}; chloroform, 3518 cm^{-1}; 1,1,1-trichloroethane, 3512 cm^{-1}; dichloromethane, 3505 cm^{-1}; 1,2-dichloroethane, 3499 cm^{-1}; acetonitrile, 3306 cm^{-1}. Chloroform interacts with pyridine *N*-oxides and the νOH···Solv. band is the most intense, while acetonitrile interacts with HPCP causing broadening of the band. The intensity of the νOH···Solv. band decreases with increasing pK_a values of the *N*-oxides. Thus, in solution the following equilibrium exists:

$$A{-}H + B \rightleftarrows AHB \quad (1)$$

When excess of base is added, the intensity of the νOH···Solv. band decreases and simultaneously absorption below 3000 cm^{-1} increases, indicating

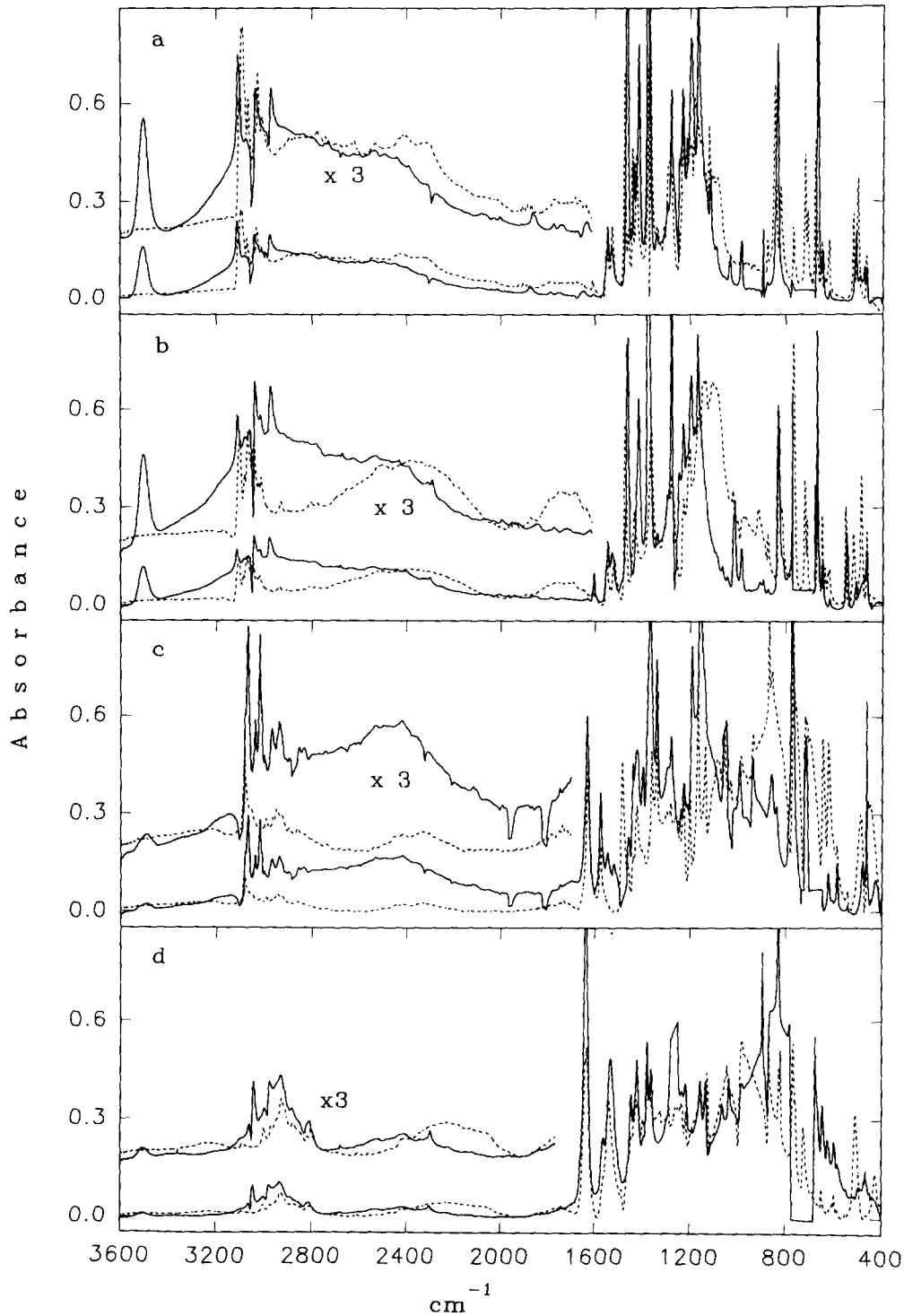

Fig. 1. FT-IR spectra of complexes (a) **1** in CH_2Cl_2, (b) **2** in CH_2Cl_2, (c) **4** in C_6H_6 and (d) **5** in CH_2Cl_2. Dotted lines denote spectra in Nujol and poly(chlorotrifluoroethylene) emulsion. Numbers refer to Table 1.

that the equilibrium is shifted towards the complex. The presence of uncomplexed HPCP with the *N*-oxide in solution is not surprising and agrees with the available formation constants; for complexes of phenols with amines, the formation constants are one order of magnitude lower than those for carboxylic acids [3(b)].

As Fig. 1. shows, the intensity of the broad

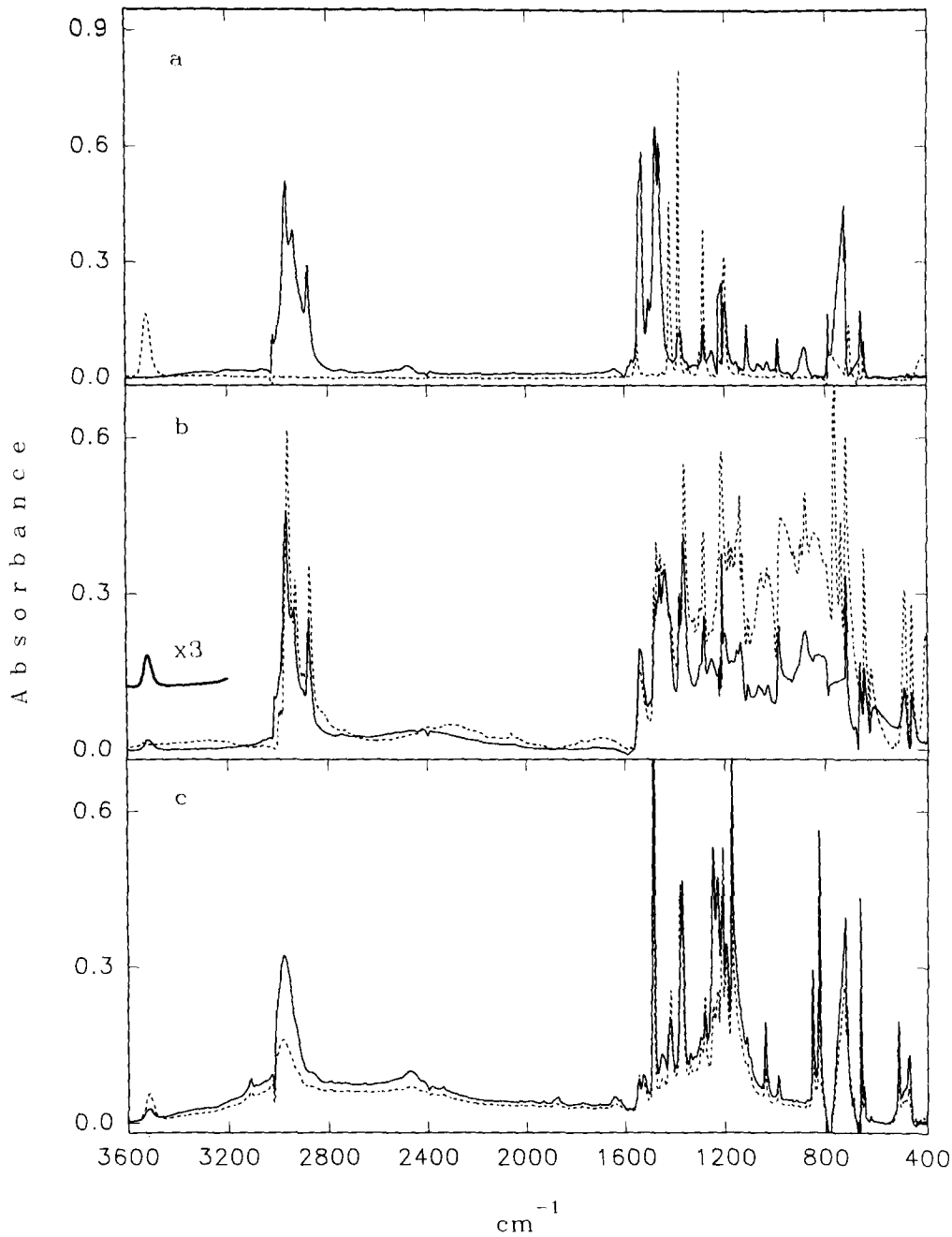

Fig. 2. FT-IR spectra of (a) $Bu_4N^+ \cdot {}^-OC_6Cl_5$ and (b) $Bu_4N^+(C_6Cl_5O \cdot H \cdot OC_6Cl_5)^-$ in $CHCl_3$ solution (——) and in Nujol and poly(chlorotrifluoroethylene) emulsion (- - - -) and (c) (——) 1 : 1 and (- - - -) 2 : 1 mixtures of 4-Me-pyridine *N*-oxide with HPCP.

absorption in solution is much weaker than in the solid state. Although this is partly caused by equilibrium (1), it seems that a shift of the absorption above 1700 cm^{-1} towards higher wavenumbers relative to the solid state strongly suggests that the hydrogen bonds in the investigated solutions are longer than those in the solid state.

All of the pyridine *N*-oxides [15] and phenols [10(a),16] form homoconjugated complexes, $(BHB)^+X^-$ and $(AHA)^-Y^+$, with comparable formation constants. Indeed, HPCP forms both a neutral salt, **6**, and an acid salt, **7**, in the solid state. The 3518 cm^{-1} band in the solution spectrum of salt **7** indicates that this salt is in equilibrium with salt **6** and HPCP (Fig. 2).

Pawlak et al. [17] investigated the complex of trimethylamine *N*-oxide with HPCP and postulated the formation of the complexes $Me_3NO^+H\ (C_6Cl_5O \cdot H \cdot OC_6Cl_5)^-$ and $(Me_3NO \cdot H \cdot ONMe_3)^+C_6Cl_5O^-$ on addition of an excess of

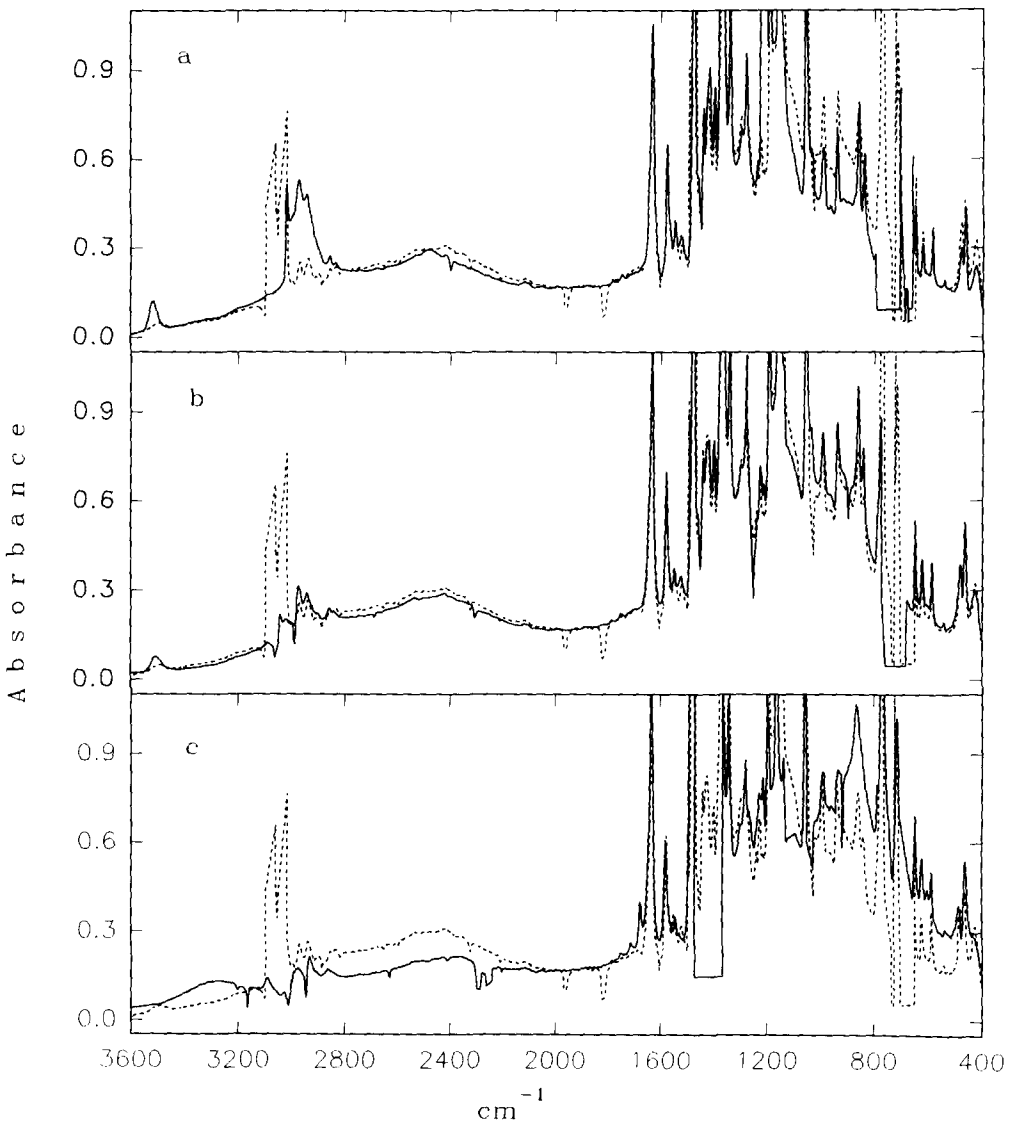

Fig. 3. Solvent effect on FT-IR spectra of complex **4** in: (a) $CHCl_3$; (b) CH_2Cl_2; (c) CH_3CN. Dotted lines denote spectra in C_6H_6.

HPCP or *N*-oxide to the equimolar complex, respectively. Lack of the broad absorption below 2000 cm^{-1} demonstrates that the homoconjugated complex is not formed in the 2:1 mixture of 4-methylpyridine *N*-oxide with HPCP (compare Figs. 2(b) and 2(c); an excess of *N*-oxides only shifts the equilibrium towards the complex side. On the contrary, the formation of homoconjugated complexes $(BHB)^+A^-$ was observed in addition of an excess of *N*-oxides to the equimolar complexes of some pyridine *N*-oxides with trifluoroacetic acid [18].

We have recently shown that the formation of homoconjugated complexes between 1:1 complexes of *N*-dodecyl-*N*,*N*-dimethylamine *N*-oxide (DDAO) with mineral and organic acids on addition of excess of DDAO depends on the acid used [19]. The stronger the interaction between $DDAO^+H$ and the anion, the smaller is the formation constant of the homoconjugated cation $(BHB)^+$. In the series of DDAO complexes with halogenoacetic acids, the formation of $(BHB)^+A^-$ decreases in the order: CF_3COOH > $CHCl_2COOH$ > $CH_2ClCOOH$ > CH_3COOH.

Only complex **4** is soluble enough in organic solvents. In benzene ($\epsilon = 2.27$), tetrachloroethylene ($\epsilon = 2.30$), chloroform ($\epsilon = 4.81$), 1,1,1-trichloroethane ($\epsilon = 7.25$), dichloromethane ($\epsilon = 8.93$) and 1,2-dichloroethane ($\epsilon = 10.37$) the spectra are very similar (Fig. 3). This suggests that the dipolar interactions between complex **4** and these solvents are similar. The structure and intensity of the broad absorption are the same within the experimental reproducibility; the centres of gravity for the total absorption in the 1700–400 cm^{-1} region in the six investigated solvents are similar, $\nu' = 1145 \pm 25$ cm^{-1}. More pronounced variation is observed in acetonitrile ($\epsilon = 35.94$) where absorption in the 2900–2100 cm^{-1} region is weaker but in the 1000–500 cm^{-1} region is stronger (Fig. 3(c)). This suggests that in acetonitrile the hydrogen bond is shorter than in less polar solvents.

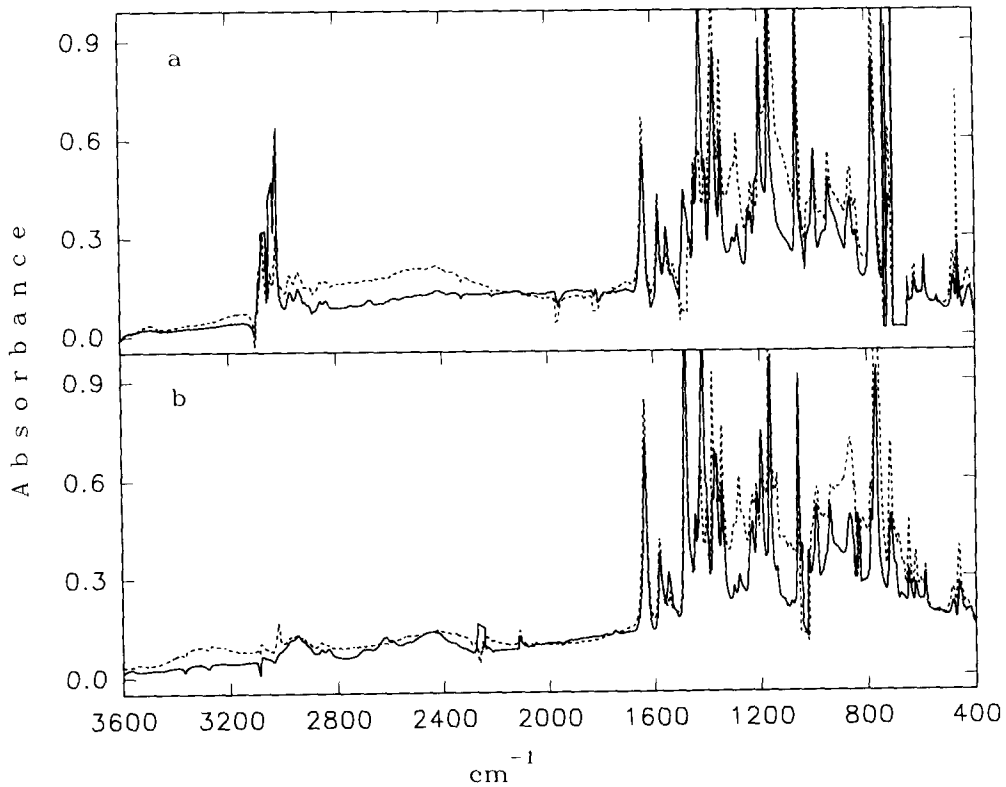

Fig. 4. FT-IR spectra of complex **4** (- - - -) and its deuterated analogue (——) in (a) C_6H_6 and (b) CD_3CN.

Similar resistance has been observed in complexes of pyridine *N*-oxides with trifluoroacetic acid and some acid salts [18,19]. This broad absorption is classified as type (ii). Absorption showing larger and linear variations with solvent polarity is classified as type (i). Absorption of type (i) has been observed in complexes of pyridines with halogenoacetic acids [1]. The type of broad absorption is related to the potential energy function. Absorption of type I is generally observed for OHN complexes where the simultaneous appearance of two kinds of species, a molecular complex (A–H ··· B) and an ionic (A^- ··· H–B^+) complex, were observed. When only one species is present absorption of type II was observed.

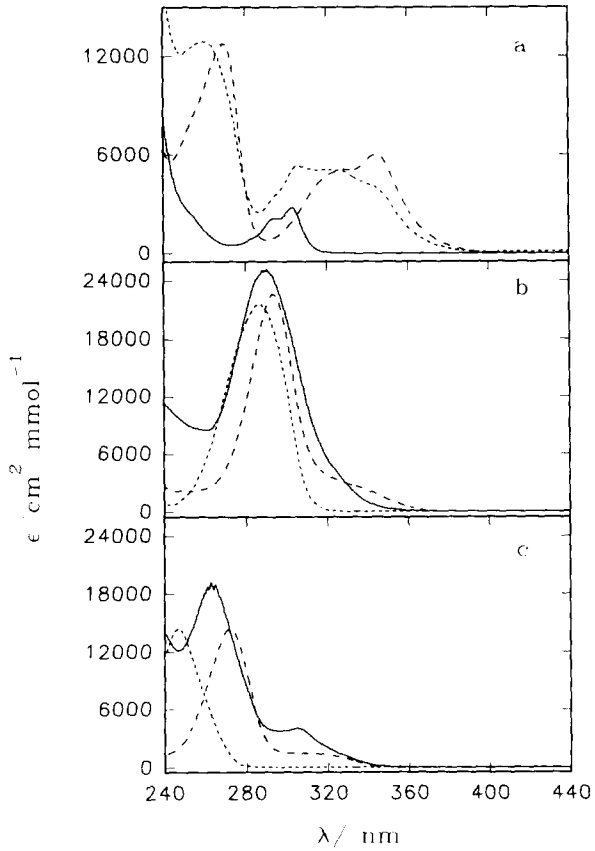

Fig. 5. UV spectra of pentachlorophenol (HPCP) and its complexes: (a) HPCP (——), salt **6** (— — —) and salt **7** (- - - -) in CH_2Cl_2; (b) complex **5** (——), 4-NMe_2-2,6-$Me_2C_5H_2NO$ (— — —) and 4-NMe_2-2,6-$Me_2C_5H_2NO$ · HCl (- - - - - -) in CH_2Cl_2; (c) complex **4** (——), 4-OMe-2,6-$Me_2C_5H_2NO$ (— — —) and 4-OMe-2,6-$Me_2C_5H_2NO$ · HCl (- - - -) in CH_3CN.

When a proton is replaced by deuterium the broad absorption becomes less intense and hence the ratio of the centres of gravity, ν'_H/ν'_D, is close to unity (Fig. 4). Theory predicts such a low isotope ratio both for asymmetrical double and quasi-single minimum potentials with sufficient anharmonicity [20]. The observed weak solvent effect and the low isotope ratio exclude prototropic equilibrium in the investigated complexes.

3.2. Ultraviolet spectra

Figs. 5–8 show selected UV-visible spectra and Table 3 lists spectroscopic data. In the spectra of HPCP only the long-wavelength band at about 303 nm with a shoulder at about 293 nm is observed (Fig. 5). Replacing the proton by N^+Bu_4 (salt **6**) caused a bathochromic shift of the absorption and two transitions at about 270 and 344 nm are observed. The short wavelength band is narrow and the long wavelength band is broad with a shoulder at about 320 nm (Fig. 5). HPCP in

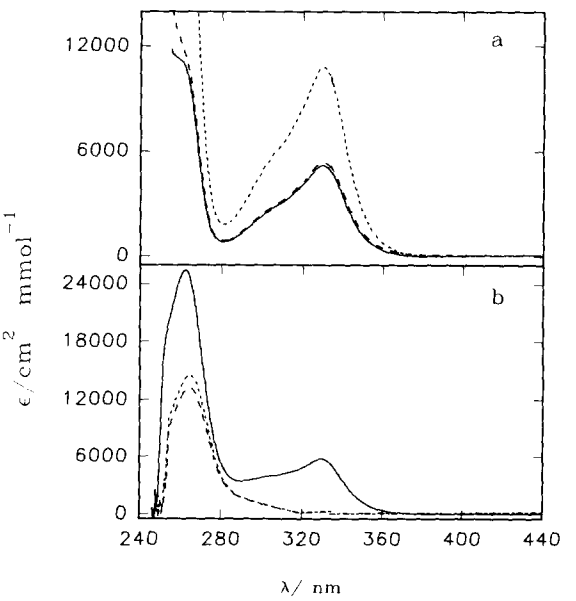

Fig. 6. UV spectra of pentachlorophenol (HPCP) and its complexes in formamide: (a) HPCP (——); salt **6** (— — —); salt **7** (- - -); (b) complex **4** (——); 4-OMe-2,6-$Me_2C_5H_2NO$ (— — —); 4-OMe-2,6-$Me_2C_5H_2NO$ · HCl (- - - -).

DMF ($\epsilon = 38.3$) is partly dissociated (a shoulder at 270 nm and a weak absorption at about 344 nm) but in formamide ($\epsilon = 111$) it is completely dissociated (spectra of HPCP and salt **6** are the same) (Fig. 6).

Absorption of salt **7** in CH_2Cl_2 can be treated as an intermediate between HPCP and salt **6**. With increasing electric permittivity of the solvent, dissociation increases and the absorption of salt **7** becomes more similar to that of salt **6**. Salt **7** in formamide is completely dissociated and a band at about 330 nm is, as expected, twice as large as that in salt **6** (Fig. 6(a)).

In 4-MeO-2,6-$Me_2C_5H_2NO$ and 4-NMe_2-2,6-$Me_2C_5H_2NO$ only one transition is observed at about 270 and 290 nm, respectively, with additional long-wavelength tails. In hydrochlorides the *N*-oxides are protonated and this produces a hypsochromic shift (Table 3; Fig. 5).

In complex **4** the long-wavelength band due to the phenol undergoes a bathochromic shift of about 2–3 nm relative to the "free" HPCP, but the long-wavelength band of the *N*-oxides is shifted about 8–10 nm to the blue relative to the free *N*-oxide and is accompanied by a hyperchromic effect (Fig. 7). In complex **5** the phenol band is hidden by the *N*-oxide absorption and the observed band is shifted about 3 nm to the blue relative to the free *N*-oxide. The magnitude of these shifts with the solvent decreases in the order CH_2Cl_2 > CH_3CN > DMF and can be explained by a specific interaction of HPCP with the solvents. Phenol forms complexes with CH_3CN and DMF; the formation constants are 4.8 ± 0.1 and 72 ± 6, respectively [3(b)]. The weak hypsochromic shift of the short-wavelength band and the absence of absorption at 340 nm exclude the formation of a hydrogen-bonded ion pair ($A^- \cdots H\text{–}B^+$).

The absorption observed in formamide solution of complex **4** is attributed to solvated *N*-oxide and dissociated phenol. Spectra of 4-MeO-2,6-$Me_2C_5H_2NO$ and its hydrochloride in formamide are practically identical. This suggests that HCl

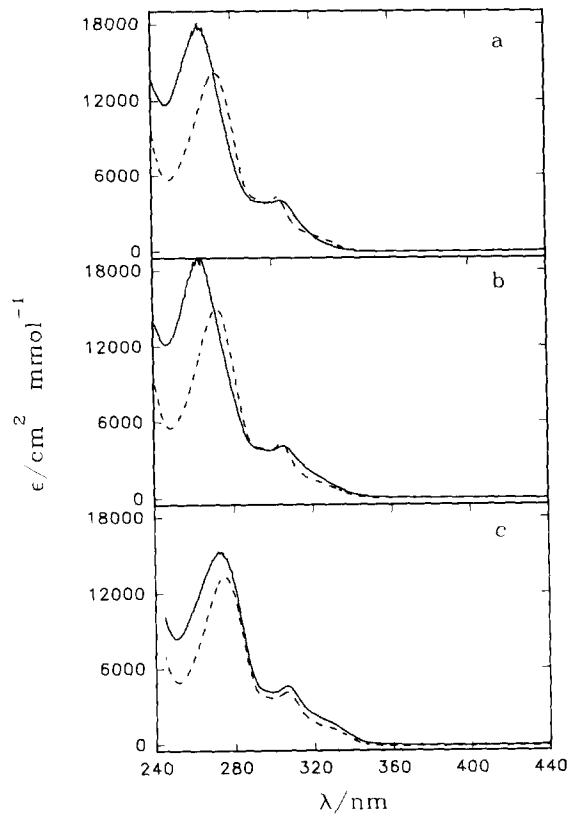

Fig. 7. UV spectra of complex **4** in: (a) CH_2Cl_2; (b) CH_3CN; (c) DMF. Dashed line is sum of absorption of 4-OMe-2,6-$Me_2C_5H_2NO$ and HPCP.

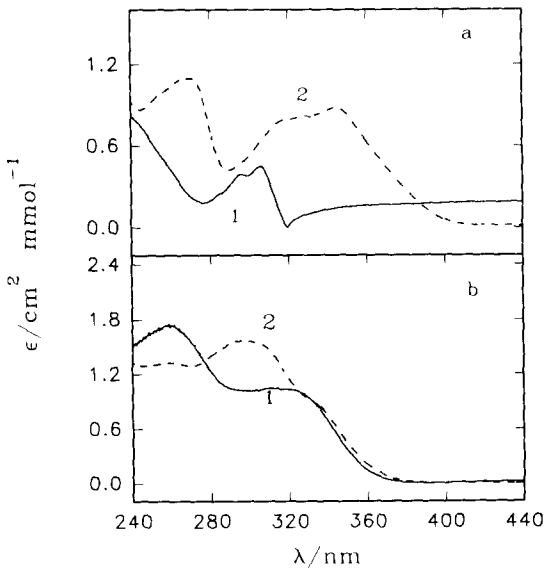

Fig. 8. UV spectra of pentachlorophenol (HPCP) and its complexes in the solid state: (a) HPCP (——); salt **6** (– – – –); (b) complex **4** (——); complex **5** (— — —).

interacts with the solvent and not with the *N*-oxide (Fig. 6(b)).

In the solid-state spectra of complexes **4** and **5** the long-wavelength band is shifted by about 6–10 nm to the red but the short-wavelength band is shifted by about 3 nm to the blue in comparison with the solution spectra (Fig. 8). The solid-state spectra of complexes **4** and **5** can be treated as intermediate between the spectra of HPCP and salt **6**.

Wolny et al. [21] investigated complexes of oxygen bases with several phenols in CCl_4. For some of these complexes, and particularly for tri-n-butylamine *N*-oxide (TBNO) with HPCP, the proton transfer equilibrium constant, $K_{PT} = 1.635$, has been estimated. Brzezinski et al. [22] postulated a prototropic equilibrium for the complex of trimethylamine *N*-oxide (TMNO) with HPCP from the IR spectrum. The proton-acceptor properties of these oxygen bases estimated from their pK_a values (4-NMe_2-2,6-$Me_2C_5H_2NO$, $pK_a = 4.75$ [23]; TBNO, $pK_a = 4.75$–5.1, value estimated [21]; TMNO, $pK_a = 4.65$ [22]) are comparable but their interactions with HPCP are different; in complexes of TBNO and TMNO proton transfer occurs. The difference may be caused partially by the excess of TBNO used by Wolny et al. [21]. An excess of base or acid changes the number of hydrogen-bonded species in solution [23].

From femtosecond–picosecond laser photolysis studies it is known that the proton transfer process is fast in the excited state of hydrogen-bonded complexes and can be described by Eq. (2) (see for example [24]):

$$(A{-}H\cdots B) \xrightarrow{h\nu} (A{-}H\cdots B)^* \xrightarrow{PT} (A^-\cdots HB^+)^* \xrightarrow{ID} [(A^-)^*_{sol} + (HB^+)_{sol}] \text{ or } [(A^-)_{sol} + (HB^+)^*_{sol}] \quad (2)$$

Table 3
UV absorption data for pentachlorophenol (HPCP) and its complexes with 4-R-2,6-dimethyl-pyridine-*N*-oxides and tetrabutylammonium salts; $c = 0.05$ mol dm^{-3} and $l = 0.0029$ cm if not stated otherwise

Compound	Benzene		CH_2Cl_2		CH_3CH		DMF		Formamide	
	λ (nm)	ε	λ (nm)	ε	λ (nm)	ε	λ (nm)	ε	λ (nm)	ε
HPCP	–		(295)	(2100)	(295)	(2120)	(297)	(2120)		
			303	2750	304	2760	305	2750	330	5550[a]
$Bu_4N \cdot PCP$	–		269	12760	268	12300	272	13450		
			(320)	(4700)	(320)	(4570)	330	5780	330	5360[a]
			344	6034	344	5726	349	6100		
$Bu_4N \cdot$ (PCPHPCP)	–		309	7250	309	6700	309	6370		
			(329)	(5640)	(327)	(5730)	(330)	(5930)	330	10796[a]
							(350)	(3950)		
4-OMe-2,6-Me_2-$C_5H_2NO \cdot$ HPCP			264	17860	263	18830	273	15250	262	25450[a]
	306	4315	305	4040	305	4080	306	4620		
							(329)	(1810)	330	5740[a]
4-OMe-2,6-Me_2-C_5H_2NO	–		272	13710	271	14450	274	12690		
			(319)	(1330)	(319)	(1350)	(327)	(1420)	264	13200[a]
4-OMe-2,6-Me_2-$C_5H_2NO \cdot$ HCl	–		–		247	14430	250	11850	264	14430[a]
4-NMe_2-2,6-Me_2-$C_5H_2NO \cdot$ HPCP	293	22000[a]	290	25200[b]	293	23800[a]	296	25280[a]	291	25530[a]
							(350)	(3820)[a]	(331)	(8280)[a]
4-NMe_2-2,6-Me_2-C_5H_2NO			293	22610[b]	293	22400[b]			290	[c]
			(336)	(2500)[b]	(336)	(2530)[b]				
4-NMe_2-2,6-Me_2-$C_5H_2NO \cdot$ HCl			223	12700[b]	223	12680[a]				
			288	21510[b]	287	22270[a]				

[a] $l = 0.1$ cm, $c \approx 5 \times 10^{-4}$ mol dm^{-3}; [b] $l = 0.0029$ cm, $c = 0.025$ mol dm^{-3}; [c] $l = 0.1$ cm, saturated solution.

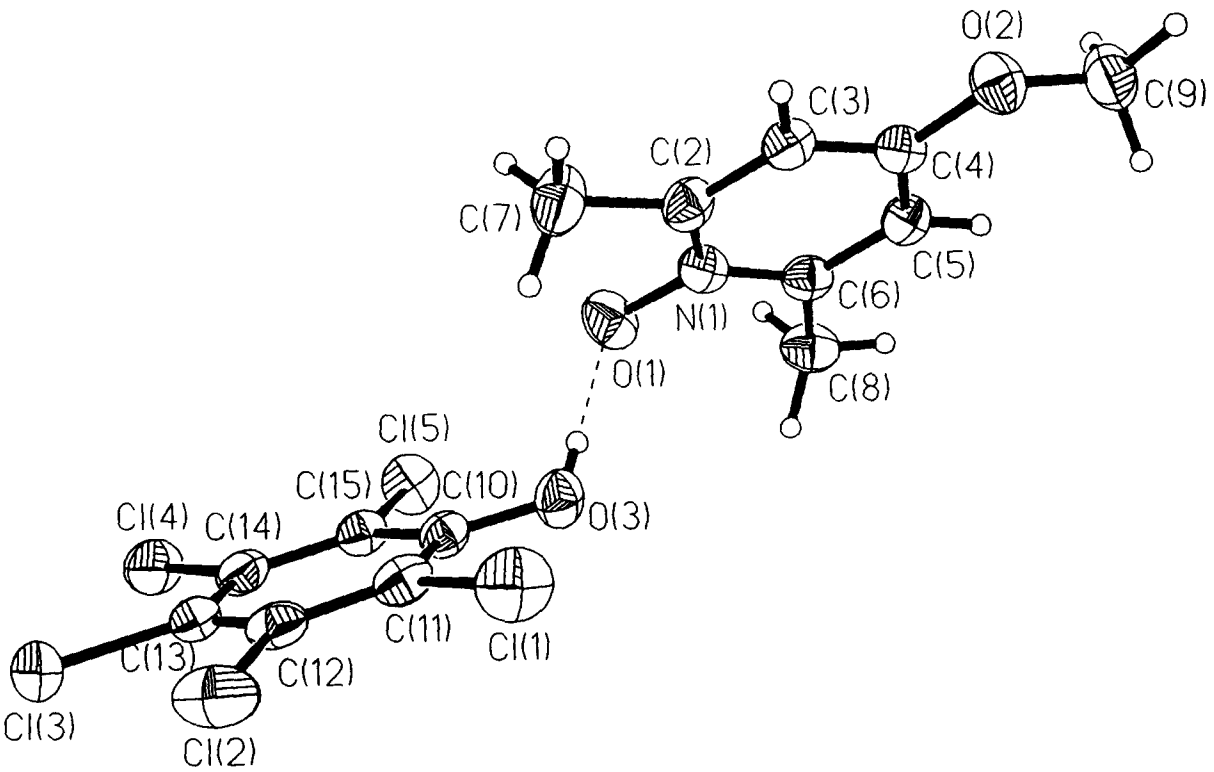

Fig. 9. Thermal ellipsoid view of the 4-methoxy-2,6-dimethylpyridine *N*-oxide complex with pentachlorophenol illustrating the mutual orientation of the two rings in the crystal and showing the labelling scheme. The thermal ellipsoids have been drawn at the 50% probability level.

This is due to the well-known fact that phenols in their ground state are much weaker acids relative to their S_1 state (see for example [25]). In UV spectroscopy absorption is due to transition between the ground and excited states and the estimated proton transfer degree in the literature is probably a total for these two states.

3.3 X-Ray diffraction studies

Displacement parameters of complex **4** are listed as supplementary data.[1] Fig. 9 shows a plot of complex **4** drawn with a Siemens program [26] and the numbering of the atoms. Atomic coordinates of complex **4** are listed in Table 4 and bond distances and angles in Table 5. Most of the bonds and angles of the phenol skeleton are very close to those in HPCP [27].

The mean C–O bond length and the mean C–C(O)–C bond angle for HPCP and its six molecular complexes are 1.332 ± 0.008 Å and $117.8 \pm 0.9°$, respectively [28]. For ten ionic complexes these values are: C–O, 1.285 ± 0.014 Å; C–C(O)–C, $114.8 \pm 0.8°$. In complex **4** both C(10)–O(3) bond and the C(11)–C(10)–C(15) angle (Table 5) are very close to those in the molecular complexes, proving that the hydrogen-bonded proton is not transferred from the HPCP to the *N*-oxide. The difference Fourier map showed that the hydrogen-bonded proton is located close to the phenolic oxygen (O(3)–H(0) = 1.04 Å; O(1)···H(0) = 1.47 Å); however, the peak height is equal to one third of the electron and hence it cannot be used as evidence of its localization. The bond length and angles of the pyridine skeleton are in the range of data for pyridine *N*-oxides [29].

[1] Supplementary data: atomic coordinates for hydrogen atoms, lists of structure factors, anisotropic thermal parameters, torsion angles and complete geometry have been deposited at the Cambridge Crystallographic Data Centre.

Table 4
Atomic coordinates ($\times 10^4$) for non-hydrogen atoms and ($\times 10^3$) for hydrogen atom, equivalent isotropic displacement coeffi-cients for non-hydrogen atoms ($Å^2 \times 10^3$) and isotropic for hydrogen atom ($Å^2 \times 10^2$)

Atom	x	y	z	U(eq)[a]
O(1)	7143(5)	2836(3)	3919(3)	83(1)
N(1)	7412(4)	4241(3)	4169(3)	61(1)
C(2)	7624(6)	5139(5)	3373(4)	66(2)
C(3)	7980(6)	6545(5)	3648(4)	62(1)
C(4)	8163(5)	7052(4)	4703(4)	56(1)
C(5)	7899(5)	6109(5)	5492(4)	61(1)
C(6)	7512(5)	4685(4)	5210(4)	60(1)
C(7)	7471(11)	4531(7)	2238(5)	95(3)
C(8)	7193(7)	3619(6)	5999(5)	80(2)
C(9)	8904(10)	9021(6)	5983(5)	93(3)
O(2)	8538(5)	8447(3)	4884(3)	74(1)
O(3)	4070(4)	2682(3)	2723(3)	70(1)
C(10)	3577(5)	1817(4)	1843(3)	55(1)
C(11)	2450(6)	2301(5)	863(4)	62(1)
C(12)	1869(5)	1427(5)	−68(4)	66(2)
C(13)	2434(6)	13(5)	−39(4)	67(2)
C(14)	3552(6)	−494(4)	929(4)	64(2)
C(15)	4114(5)	391(4)	1963(4)	56(1)
Cl(1)	1788(2)	4053(1)	827(2)	98(1)
Cl(2)	413(2)	2051(2)	−1265(1)	102(1)
Cl(3)	1743(2)	−1077(2)	−1196(1)	109(1)
Cl(4)	4256(2)	−2232(1)	994(2)	96(1)
Cl(5)	5485(2)	−228(1)	3084(1)	80(1)
H(0)	527	249	333	16(3)

[a] Equivalent isotropic U defined as one-third of the trace of the orthogonalized U_{ij} tensor. B_{iso} for hydrogen atom.

Table 5
Molecular geometry of complex **4** (4-methoxy-2,6-dimethyl-pyridine *N*-oxide with pentachlorophenol)

Bond	Distance (Å)	Bond angle	Value (deg)
O(1)–N(1)	1.349(4)	O(1)–N(1)–C(2)	118.9(4)
N(1)–C(2)	1.364(6)	O(1)–N(1)–C(6)	118.1(4)
N(1)–C(6)	1.346(6)	N(1)–C(2)–C(3)	118.5(4)
C(2)–C(3)	1.361(6)	N(1)–C(2)–C(7)	118.5(4)
C(2)–C(7)	1.498(8)	N(1)–C(6)–C(5)	118.5(4)
C(3)–C(4)	1.369(6)	N(1)–C(6)–C(8)	118.3(4)
C(4)–O(2)	1.338(5)	C(2)–N(1)–C(6)	123.0(4)
C(4)–C(5)	1.397(6)	C(2)–C(3)–C(4)	121.2(4)
C(5)–C(6)	1.382(6)	C(3)–C(2)–C(7)	123.0(5)
C(6)–C(8)	1.489(8)	C(3)–C(4)–O(2)	116.2(4)
O(2)–C(9)	1.423(7)	C(3)–C(4)–C(5)	118.7(4)
C(10)–O(3)	1.322(5)	C(4)–C(5)–C(6)	120.0(4)
C(10)–C(11)	1.385(6)	O(3)–H(0)–O(1)	152.3
C(10)–C(15)	1.405(5)	H(0)–O(1)–N(1)	112.1
C(11)–C(12)	1.378(6)	C(10)–O(3)–H(0)	119.0
C(12)–C(13)	1.399(7)	C(10)–C(11)–C(12)	121.8(4)
C(13)–C(14)	1.379(6)	C(11)–C(10)–O(3)	119.9(4)
C(14)–C(15)	1.386(6)	C(11)–C(10)–C(15)	117.6(4)
Cl(1)–C(11)	1.725(5)	C(12)–C(13)–C(14)	119.3(4)
Cl(2)–C(12)	1.727(4)	C(13)–C(14)–C(15)	120.3(4)
Cl(3)–C(13)	1.713(5)	C(14)–C(15)–C(10)	121.1(4)
Cl(4)–C(14)	1.721(4)	Cl(1)–C(11)–C(10)	118.0(3)
Cl(5)–C(15)	1.721(4)	Cl(2)–C(12)–C(11)	120.5(4)
O(1)–O(3)	2.439(6)	Cl(3)–C(13)–C(12)	120.3(3)
O(3)–H(0)	1.04	Cl(4)–C(14)–C(13)	120.5(4)
O(1)–H(0)	1.47	Cl(5)–C(15)–C(10)	117.9(3)

In complex **4** the O(3)···O(1) distance is 2.439(6) Å, while the hydrogen bond length is 2.53 Å and the O(3)–H···O(1) angle is 152.3°. This indicates that the hydrogen bond in complex **4** is much shorter than that in complexes of HPCP with nitrogen heterocycles; the shortest NHO bond is in the complex of 4-methylpyridine with HPCP (N···O distance is 2.552(4) Å; NHO angle is 170(5)°) [30]. This is not surprising, since O···O distances are generally shorter than N···O distances. The hydrogen bonds also vary with the proton-donor and proton-acceptor properties of phenols and *N*-oxides. In complexes of 4-nitro-pyridine *N*-oxide with 3-aminophenol [9(c)] and 4-nitrophenol [9(d)] the O···O distances are 2.696(3) and 2.618 Å and the O–H–O angles are 175(4) and 179.8°, respectively.

The conformation of complex **4** may be described by essentially four planes, whose equations of the form $ax + by + cz = d$ referred to crystal coordinates are: plane 1, through the six atoms of the pyridine ring with $a = 7.334$, $b = -1.936$, $c = -0.075$ and $d = 4.572$; plane 2, through six carbon atoms of the HPCP ring with $a = 7.072$, $b = 2.627$, $c = -6.819$ and $d = 1.748$; plane 3, through O(3), O(1) and N(1) atoms with $a = -4.508$, $b = -1.229$, $c = 11.759$ and $d = 1.041$; plane 4 through atoms C(9), O(2), C(4) with $a = 7.545$, $b = -1.827$, $c = -1.559$ and $d = 4.137$. The dihedral angles between these planes are: 1 to 2, 43.5°; 1 to 3, 108.0°; 2 to 3, 143.5°; 1 to 4, 6.8°.

The stacking of the pyridine *N*-oxide rings in columns parallel to the *X*-axis is found in the structure of complex **4** (Fig. 10).

4. Conclusions

In complex **4** the O···O distance is 2.439(6) Å and the OHO bond angle is 152.3° and the hydrogen-bonded proton is close to the phenol molecule. The IR spectra show that in solution the following equilibrium exists: AH + B ⇄ A–H···B. The amount of uncomplexed species decreases with an increase of the proton-acceptor property of the *N*-oxide and increases with dilution. Solvent effects on the IR spectra are explained in terms of dipolar and specific interactions.

The UV spectra demonstrate that solvents interact strongly with HPCP, *N*-oxides and the complexes. In solutions with $\epsilon \geqslant 37.5$ HPCP becomes partly dissociated and in formamide ($\epsilon = 111$) it is completely dissociated. Formamide is a much stronger proton-acceptor than the investigated pyridine *N*-oxides. All the investigated complexes exist as a molecular complexes (A–H···B). Although 4-dimethylamino-2,6-dimethylpyridine *N*-oxide, TBNO and TMNO have similar pK_a values, their interactions with HPCP are very different. In the case of TBNO and TMNO an ionic complex ($A^- \cdots H\text{–}B^+$) was found. The difference is probably caused by an excess of TBNO added to the equimolar complex.

The broad absorption in the investigated complexes is classified as type (ii) because it is resistant to the solvent effect. The hydrogen bonds in the investigated complexes of HPCP with pyridine *N*-oxides can be described by a strongly asymmetrical double minimum (complexes **1**–**3**) and by a quasi-single minimum (complexes **4** and **5**).

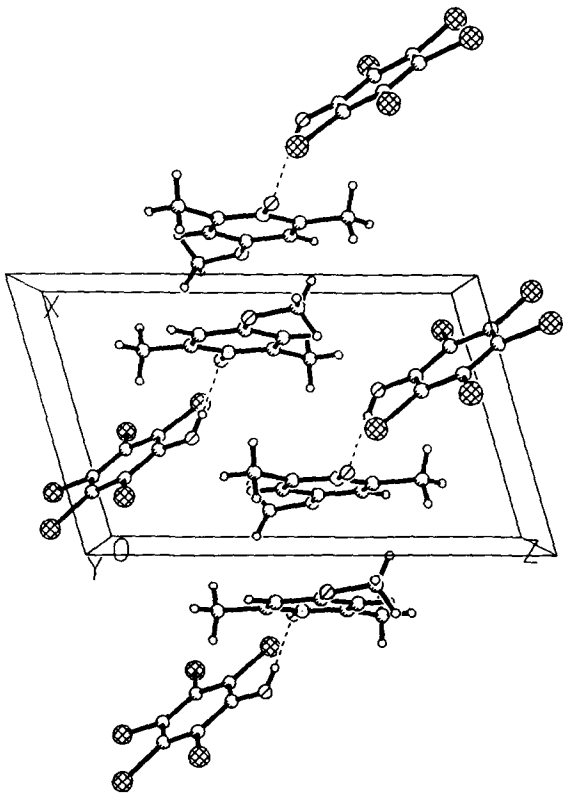

Fig. 10. The molecular packing of complex **4** in the unit cell.

Acknowledgement

We thank the State Committee for Scientific Research Grant (KBN/2P303 06907).

References

[1] Z. Dega-Szafran and M. Szafran, Heterocycles, 37 (1994) 627.

[2] (a) L. Sobczyk, H. Engelhardt and K. Bunzl, in P. Schuster, G. Zundel and C. Sandorfy (Eds.), The Hydrogen Bond: Recent Development in Theory and Experiments, Vol. 3, North Holland, Amsterdam, 1976, p. 937.
(b) Th. Zeegers-Huyskens and P. Huyskens, in H. Ratajczak and W.J. Orville-Thomas (Eds.), Molecular Interactions, Vol. 2, Wiley, Chichester, 1981, p. 1.
(c) I. Majerz, Z. Malarski and T. Lis, J. Crystallogr. Spectrosc. Res., 19 (1989) 349.

[3] (a) E.N. Guryanova, I.P. Goldshtein and T.I. Perepelkova, Usp. Khim., 45 (1976) 1568.
(b) M.D. Joesten and L.J. Schaad, Hydrogen Bonding, Marcel Dekker, NY, 1974.
(c) J.N. Spencer, J.C. Andrefsky, A. Grushov, J. Naghdi, L.M. Patti and J.F. Trader, J. Phys. Chem., 91 (1987) 1673.
(d) J. Małecki, in H. Ratajczak and W.J. Orville-Thomas (Eds.), Molecular Interactions, Vol. 2, Wiley, Chichester, 1982, p. 183.

[4] S. Bratos, H. Ratajczak and P. Viot, in J.C. Dore and J. Teixeira (Edsd.), Hydrogen-Bonded Liquids, Kluwer Academic Publishers, The Netherlands, 1991, p. 221.

[5] D. Borgis, G. Tarjus and H. Azzouz, J. Chem. Phys., 97 (1992) 1390, and references cited therein.

[6] G. Zundel, in P. Schuster, G. Zundel and C. Sandorfy

(Eds.), The Hydrogen Bond: Recent Development in Theory and Experiments, Vol. 1, North Holland, Amsterdam, 1976, p. 164.
[7] R. Janoschek, E.G. Weidemann, H. Pfeiffer and G. Zundel, J. Am. Chem. Soc., 94 (1972) 2387.
[8] Y. Guissani, B. Guillot and S. Bratos, J. Chem. Phys., 88 (1988) 5850.
[9] (a) T. Gramstad, Spectrochim. Acta, 19 (1963) 829.
(b) N. Kulevsky and L. Lewis, J. Phys. Chem., 76 (1972) 3502.
(c) J.R. Lechat, R.H.A. Santos and W.A. Bueno, Acta Crystallogr., Sect. B, 37 (1981) 1468.
(d) R.M. Fuquen, R.H.A. Santos and J.R. Lechat, J. Cryst. Spectrosc., 22 (1992) 201.
[10] (a) E.P. Serjeant and B. Dempsey, Ionization Constants of Organic Acids in Aqueous Solution (IUPAC Chemical Data Series no. 23), Pergamon Press, Oxford, 1979.
(b) Z. Pawlak and R.G. Bates, J. Chem. Thermodyn., 14 (1982) 1035.
[11] DATARED, User's manual, Appendix 1, KUMA Diffraction, Wrocław, Poland, 1989.
[12] G.M. Sheldrick, SHELXS86, Program for the solution of crystal structures, University of Göttingen, Germany, 1986.
[13] G.M. Sheldrick, SHELX-76, Program for Crystal Structure Determination, University of Cambridge, Cambridge, 1976.
[14] International Tables for X-ray Crystallography, Vol. 4, Kynoch Press, Birmingham, 1974.
[15] (a) M. Szafran and Z. Dega-Szafran, J. Mol. Struct., 99 (1983) 189.
(b) B.A. Korolev, L.A. Osmolovska and K.M. Dumaev, Zh. Obshch. Khim., 49 (1979) 898.
[16] (a) Z. Pawlak, B. Nowak and M. Fox, J. Chem. Soc., Faraday Trans. 1, 78 (1982) 2157.
(b) Z. Pawlak and J. Magoński, J. Chem. Soc., Faraday Trans. 1, 78 (1982) 2807.
[17] Z. Pawlak, M. Tusk, S. Kuna, F. Strohbusch and M.F. Fox, J. Chem. Soc., Faraday Trans. 1, 80 (1984) 1757.
[18] Z. Dega-Szafran, M. Grundwald-Wyspiańska and M. Szafran, J. Chem. Soc., Faraday Trans., 87 (1991) 3825.
[19] B. Brycki and M. Szafran, J. Mol. Liq., 59 (1994) 83; J. Mol. Struct., 239 (1990) 1.
[20] Y. Guissani and H. Ratajczak, Chem. Phys., 62 (1981) 319.
[21] R. Wolny, A. Koll and L. Sobczyk, J. Phys. Chem., 89 (1985) 2053.
[22] B. Brzezinski, B. Brycki, G. Zundel and T. Keil, J. Phys. Chem., 95 (1991) 8598.
[23] P. Barczyński and M. Szafran, J. Chem. Soc., Faraday Trans., 90 (1994) 2489.
[24] (a) H. Miyasaka and N. Mataga, in N. Mataga, T. Okada and H. Masuhara (Eds.), Dynamics and Mechanisms of Photoinduced Transfer and Related Phenomena, Elsevier Science Publishers, B.V., 1992.
(b) H. Miyasaka, A. Tabata, K. Kamada and N. Mataga, J. Am. Chem. Soc., 115 (1993) 7335.
(c) S. Sato, T. Ebata and N. Mikami, Spectrochim. Acta, Part A, 50 (1994) 1413.
[25] C. Jouvet, C. Lardeux-Dedonder, M. Richard-Viard, D. Solgadi and A. Tramer, J. Phys. Chem., 94 (1990) 5041.
[26] XP Siemens Analytical X-Ray Instruments Inc., Madison, Wisconsin, USA, 1993.
[27] T. Sakuri, Acta Crystallogr., 15 (1962) 1164.
[28] F.H. Allen and O. Kennard, CSD; Chemical Design Automation News, 1993, 8.1.31–37.
[29] J.F. Chiang and J.J. Song, J. Mol. Struct., 96 (1982) 151.
[30] Z. Malarski, I. Majerz and T. Lis, J. Mol. Struct., 158 (1987) 369.